

Supplemental info

The PDF file includes:

Fig. S1. Analysis of CAR expression at the cell surface.

Fig. S2. Transient depletion of CD19⁺ B cells from one NZB/W mouse.

Fig. S3. Immunofluorescence images of representative glomeruli from CAR T cell-treated and control MRL-lpr mice.

Fig. S4. Comparison of alopecia and skin lesions between CAR T cell-treated and negative control MRL-lpr mice.

Fig. S5. Analysis of CAR T cell cytotoxicity in vivo.

Fig. S6. qPCR of transcripts expressed in sorted CD8⁺ T cells.

Fig. S7. Reverse transcription qPCR of CAR RNA in bone marrow and spleen of CD19⁺ depleted and CD19⁺ intact NZB/W mice.

Fig. S8. Typical gating strategy.

Table S1. Comparison of viral vectors used to transduce T cells.

Table S2. List of oligonucleotide primers used for RT-PCR.

Other Supplementary Material for this manuscript includes the following:

(available at www.sciencetranslationalmedicine.org/cgi/content/full/11/482/eaav1648/DC1)

Table S3 (Microsoft Excel format). CD4⁺ T cell subsets.

Data file S1 (Microsoft Excel format). Primary data.

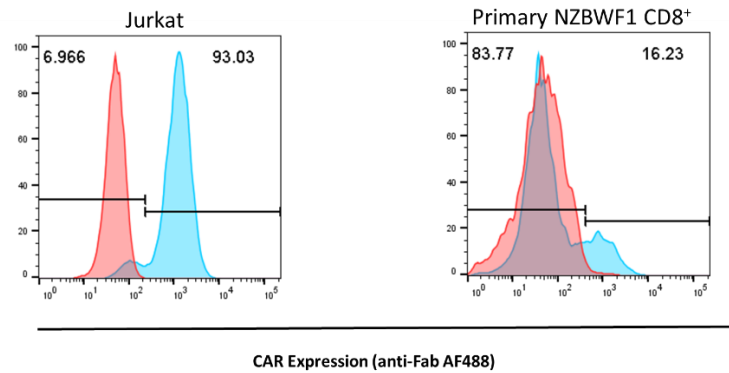
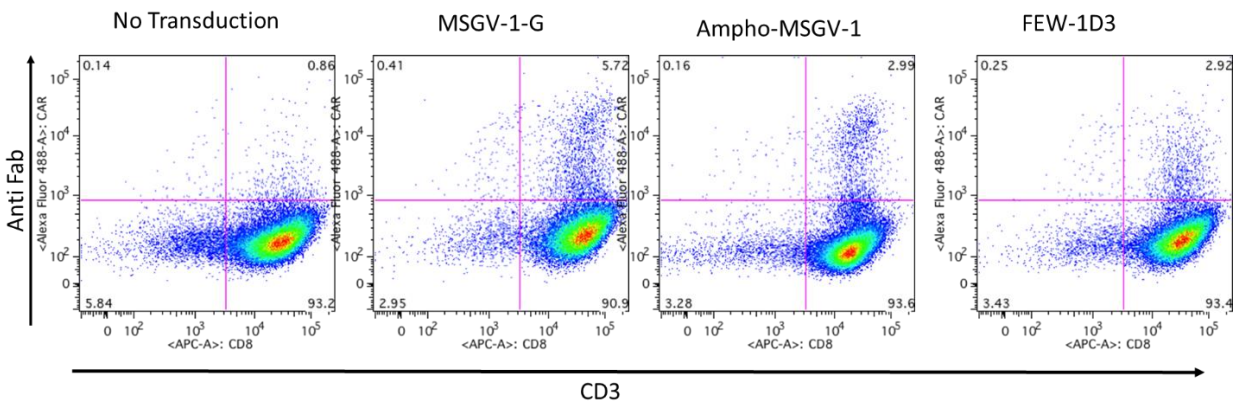
A**B**

Fig. S1. Analysis of CAR expression at the cell surface. (A) Jurkat cells were transduced with the Amphotropic 1D3 MSGV-1 retrovirus (A-MLV) and assayed at 72 h after transduction. The expression was assessed with a goat-anti-rat Fab AF488 conjugate (blue histogram). Mock-transduced, stained cells are shown in the red histogram. Populations of purified splenic CD8⁺ T cells from an NZB/W mouse following transduction with A-MLV are shown on the right. (B) Splenic CD8⁺ T cells from a second NZB/W mouse were transduced with MSGV-1-G, Ampho-MSGV-1, FEW-1D3 or mock-transduced and CAR expression on CD3⁺ cells was analyzed at 72 h post transduction.

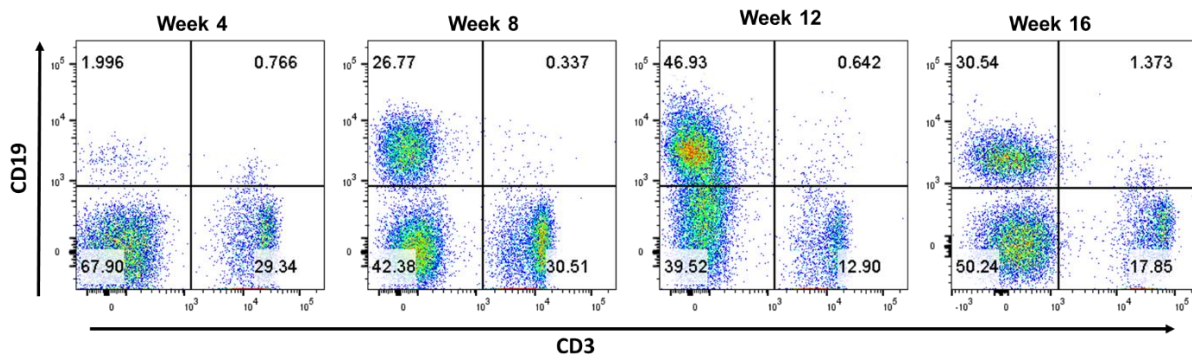


Fig. S2. Transient depletion of CD19⁺ B cells from one NZB/W mouse. One mouse that initially showed effective CD19⁺ B cell depletion was assayed for expression of CD19⁺ B cells at 2, 3 and 4 months after treatment with MSGV-1-CAR retrovirus.

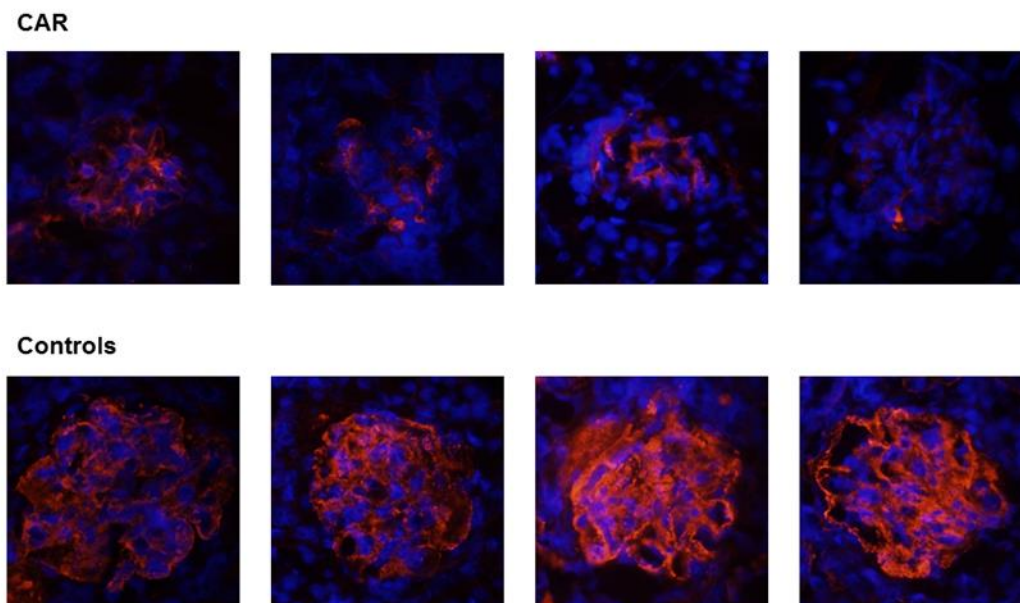


Fig. S3. Immunofluorescence images of representative glomeruli from CAR T cell-treated and control MRL-lpr mice. Kidneys were dissected from CAR T cell-treated and control MRL-lpr mice at necropsy, flash-frozen in OCT in a dry ice-methanol bath, and sectioned by cryostat. Immune deposits were imaged with anti-mouse IgG labeled with AF546 and counterstained with DAPI. At least 3 sections with over 100 glomeruli were examined per mouse and representative glomeruli are shown in the figure.

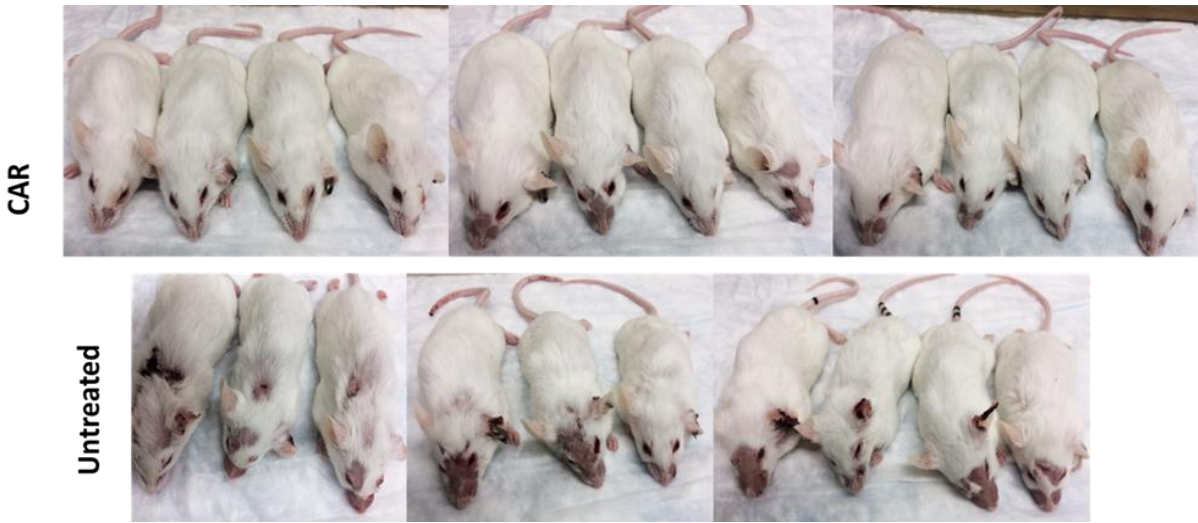


Fig. S4. Comparison of alopecia and skin lesions between CAR T cell-treated and negative control MRL-lpr mice. CAR T cell-treated mice and age-matched control mice were analyzed for progressive alopecia, skin lesions and scarring on faces, ears, necks, and the tips of their tails.

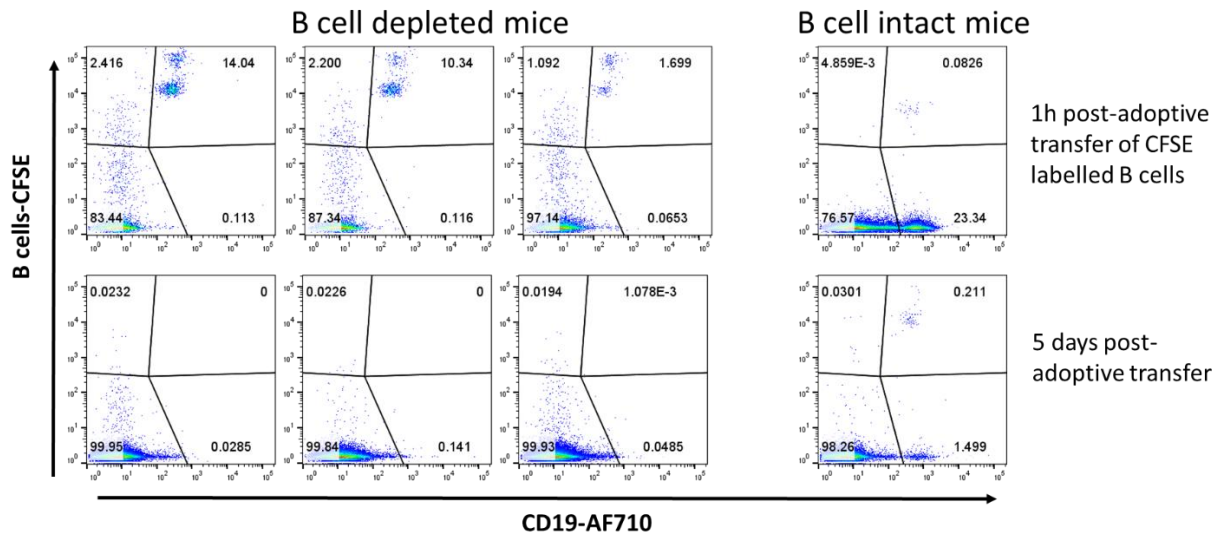
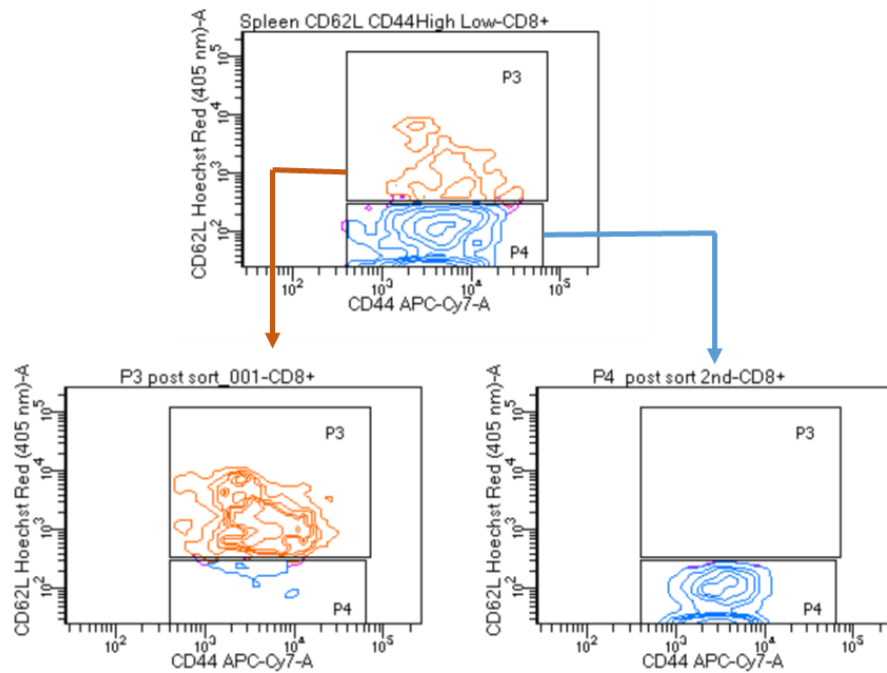


Fig. S5. Analysis of CAR T cell cytotoxicity in vivo. NZB/W mice that were either CD19⁺ B cell depleted or mock-treated were injected with 2.5×10^7 splenic B cells that had been CFSE labeled for 20 min before administration. At 1 h post and 5 h after injection, all mice were bled to identify CFSE labeled CD19⁺ B cells by flow cytometry.

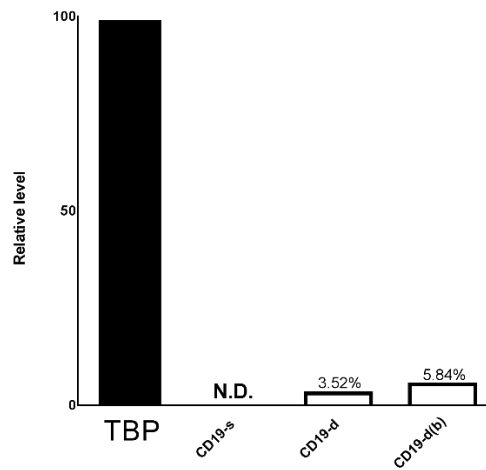


TBP	CD3e	1D3 (CAR)
27.09	24.56	31.10
27.03	24.74	31.72
26.92	23.91	31.30
26.93	23.24	32.34
27.02	23.13	32.69
26.95	23.45	32.04

Fig. S6. qPCR of transcripts expressed in sorted CD8⁺ T cells. Splenic CD8⁺ T cells were sorted according to surface CD62L and CD44 expression into a high (P3) and low-expressing population (P4). Post-sort analysis was performed to examine separation of the two populations. RNA was extracted from the sorted T cells with Trizol and processed, as described in Methods, to prepare cDNA. Quantitative PCR was performed in triplicate, yielding values for the crossing point of the amplification cycle, the cycle where each reaction first rises above background, a measure of the amount of target that was present at the beginning of the reaction. The table displays the

cycle numbers of separate wells in a 96 well plate in which TATA-binding factor (TBP) and CD3e were used as normalization standards. This experiment represents data using a single CAR T cell-treated mouse spleen that was used for flow sorting and yielded two preparations of cDNA.

A



B

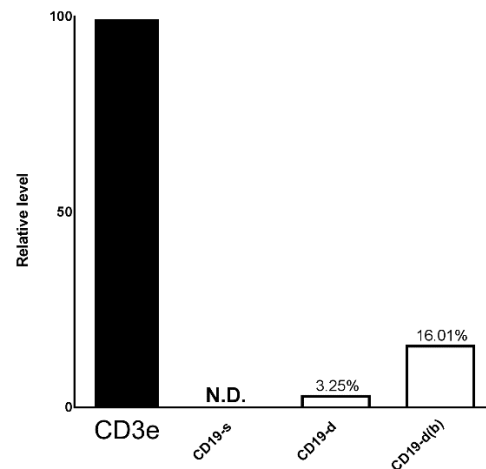


Fig. S7. Reverse transcription qPCR of CAR RNA in bone marrow and spleen of CD19⁺ depleted and CD19⁺ intact NZB/W mice. Total RNA was prepared by Trizol treatment from the (A) spleen and (B) bone marrow of 2-3 mice per group and converted to cDNA prior to q-PCR. In addition, tissues were prepared from mice that had received syngeneic B cell infusions 5 days prior to euthanasia. As was done in Figure S6, we used TBP or CD3e to normalize signals. The q-PCR

data were converted to relative levels of cDNA by setting TBP or CD3e cycle numbers as equal to 100% expression in each tissue.

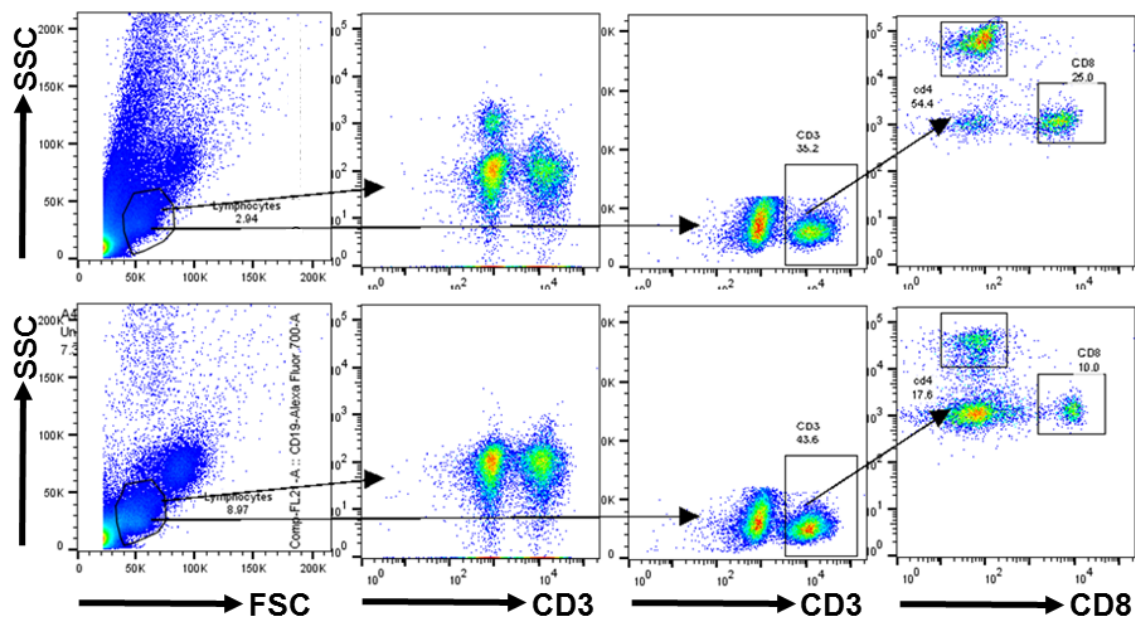


Fig. S8. Typical gating strategy. Starting from blood (left panel), lymphocytes were identified by forward and side scatter, divided according to anti-CD3 and anti-CD19 reactivity, and subsequently separated into CD4 and CD8 positive populations. Top panels are from a control MRL-lpr mouse, bottom panels from a CAR T cell-treated MRL-lpr mouse.

Table S1. Comparison of viral vectors used to transduce T cells.

Vector	Transgene	Promoter	Viral Particle	Pseudotype	CAR T cell efficiency
A-MLV	1D3-28-zeta-mut1-3	MSCV	MLV	Amphotropic	8/10
G-MLV	1D3-28-zeta-mut1-3	MSCV	MLV	VSV-G	4/9
G-LV	1D3-28-zeta-mut1-3	EF-1 α	LV	VSV-G	2/10

A-MLV, amphotropic murine leukemia virus; VSV, vesicular stomatitis virus; VSV-G, VSV with G membrane glycoprotein; G-MLV, MLV with VSV-G glycoprotein pseudotype; G-LV, lentivirus with VSV-G pseudotype; CAR T cell efficiency, number of NZB/W mice with B cell depletion over total number of mice infused with the specified transduced CD8 T cells.

Table S2. List of oligonucleotide primers used for RT-PCR.

Name of Oligonucleotide	Sequence	Detection
CD19-A L. primer	gagaggcacgtgaaggca	Probe 21
CD19-A R. primer	ggcatctagcacttgacgtc	
CD19-B L. primer	ctgacgacctagaaccagca	Probe 12
CD19-B R. primer	tggacctaacgaagtccag	
C Kappa L. primer	aaaatggcgtcctgaacagt	Probe 56
C Kappa R. primer	ctgctcatgctgtaggtgct	
Tnfrsf13b L. primer	tgtctcctgtgcactgacc	Probe 106
Tnfrsf13b R. primer	tgctctttcggcaattgat	
Tnfrsf17 L. primer	cagtgttccacagtgaatatttg	Probe 84
Tnfrsf17 R. primer	ccttctactgaactggcagc	
C Lambda L. Primer	caagtctcgccatcagtca	Probe 6
C Lambda R. Primer	acaccagtgtggccttgta	
CXCR3 L. Primer	acaagtgccaaggcagag	Probe 27
CXCR3 R. Primer	ggcatctagcacttgacgtt	
CXCR4 L. Primer	tggaaccgatcagtgtgagt	Probe 38
CXCR4 R. Primer	ggcaggaagatcctattga	
28zetaJXNFWD (1D3)	gacttcgccgctacaga	Probe 21
28zetaJXNREV (1D3)	tcgttgaacagctggttg	
Cd3e set 1FWD	cagcctcaaagaaaaacacgta	Probe 10
Cd3e set 1Rev	gatgattatggctactgctgtca	